

Chance-Constrained MPC for Voronoi-based Multi-Agent System Deployment^{*}

Thomas Chevet^{*} Cristina Stoica Maniu^{*} Cristina Vlad^{*}
Youmin Zhang^{**} Eduardo F. Camacho^{***}

^{*} *Université Paris-Saclay, CNRS, CentraleSupélec, Laboratoire des signaux et systèmes, 91190, Gif-sur-Yvette, France. (e-mail:*

{thomas.chevet, cristina.stoica, cristina.vlad}@12s.centralesupelec.fr)

^{**} *Department of Mechanical, Industrial and Aerospace Engineering, Concordia University, 1455 Blvd. de Maisonneuve, Montréal, QC H3G 1M8, Canada. (e-mail: ymzhang@encs.concordia.ca)*

^{***} *Departamento de Ingeniería de Sistemas y Automática, Universidad de Sevilla, Camino de los Descubrimientos, 41092 Sevilla, Spain. (e-mail: efcamacho@us.es)*

Abstract: This paper proposes a new chance-constrained model predictive control (CCMPC) algorithm with state estimation applied to the two-dimensional deployment of a multi-vehicle system where each agent is subject to process noise and measurement noise. The bounded convex area of deployment is partitioned into time-varying Voronoi cells defined by the position of each agent. Due to the presence of noise in the system model, stochastic constraints appear in the model predictive control problem. The proposed decentralized robust CCMPC algorithm drives the multi-agent system into a static Chebyshev configuration where each agent lies on the Chebyshev center of its Voronoi cell. Simulation results show the effectiveness of the proposed control strategy on a fleet of quadrotors subject to wind perturbations and measurement noise.

Copyright © 2020 The Authors. This is an open access article under the CC BY-NC-ND license (<http://creativecommons.org/licenses/by-nc-nd/4.0>)

Keywords: Multi-agent systems, Decentralized control, Model predictive control

1. INTRODUCTION

To carry out monitoring or search missions, a multi-agent system (MAS) composed of unmanned vehicles can be deployed over a bounded convex area (Cortes et al., 2004). Several solutions exist for the deployment problem (Schwager et al., 2011) but often rely on a dynamic Voronoi tessellation (Voronoi, 1908) of the area of interest. The objective is usually to drive the MAS into a centroidal Voronoi configuration where the objective of each agent is to reach the *center of mass* of the Voronoi cell (Sharifi et al., 2015) or into a Chebyshev configuration where the objective is the *Chebyshev center* (Nguyen et al., 2017; Hatleskog et al., 2018; Chevet et al., 2020) of the cell, which is often less complex to compute than the center of mass. In this context, the Voronoi cells and objective points are time-varying due to the movement of the agents which are constrained to remain inside their cells. The control algorithm then has to drive each agent to its objective under this time-varying movement constraint. Generally, the literature deals with the nominal case, i.e. uncertainties/perturbations are not considered. However, real systems are subject to perturbations (e.g. wind gusts)

^{*} The authors acknowledge the LIA of the CNRS on *Information, Learning and Control*, MEECOD project (“Moderniser l’Enseignement par l’Expérimentation sur la COordination de Drones”) supported by UPSaclay, the Natural Sciences and Engineering Research Council of Canada, MEyC Spain (contract DPI2016-76493-C3-1-R), the European Research Council and the UE ERDF (Advanced Grant OCONTSOLAR, Project ID: 789051).

and noises (e.g. measurement noise from sensors). The perturbations acting on the system can be modeled using deterministic or stochastic approaches. The deterministic approach requires a model of the perturbation while the stochastic approach only requires a mean and a covariance. In order to deal with these stochastic perturbations, several control methods have been proposed for a single agent, such as H_∞ (Ugrinovskii, 1998) or optimal control (Petersen et al., 2000), and for several agents, such as consensus (Ma et al., 2017) or predictive control (Dai et al., 2017).

Model predictive control (MPC) is used for a wide variety of systems dealing with constraints, uncertainties, etc. MPC can also be used for the control of a multi-agent system either in a centralized, distributed or decentralized way. If the system is subject to bounded perturbations, robust MPC strategies have been developed (Limon et al., 2010) in order to further guarantee the feasibility and stability properties for a simple system. However, if these perturbations have a stochastic nature and an unbounded support such as normally distributed noises, the classical deterministic robust MPC strategies will be too conservative. To handle this situation, several stochastic MPC algorithms have been proposed to control a single system (Farina et al., 2016) or a multi-agent system (Dai et al., 2017) subject to perturbations and probabilistic constraints. However, these methods often rely on a known bound for the perturbation and fixed constraints over time.

In this paper, a MAS composed of several unmanned vehicles is deployed inside a convex bounded two-dimensional

polyhedral area. Each agent is subject to modeling errors and perturbations, which are represented respectively by the covariance and the mean of a process noise, as well as measurement noise, both with unknown bounds. At each time instant, each agent computes its Voronoi cell based on the knowledge of the other agents' positions. Each agent is also constrained to remain inside its cell, which can be formulated as an optimization problem subject to time-varying constraints. In this way, the agents are subject to time-varying constraints. In (Gavilan et al., 2012), the authors propose a chance-constrained MPC (CCMPC) algorithm able to deal with time-varying constraints and process noise with unknown bounds for a single system. The current paper extends the result of (Gavilan et al., 2012) to the Voronoi-based deployment of a multi-agent system subject to process and measurement noise, where the full state information is not available. Due to the noises considered in the agents' dynamical model, stochastic constraints appear in the optimization problem. These stochastic constraints are transformed into algebraic constraints by computing a bound ensuring that the constraints are satisfied for almost all possible Gaussian noise signals. Each agent uses the CCMPC algorithm to track the Chebyshev center of its Voronoi cell and the MAS converges to a static Chebyshev configuration. The contribution of this paper covers: 1) the extension of the method proposed in (Gavilan et al., 2012) when the estimation of the state has to be performed; 2) the application to the Voronoi-based deployment of a MAS subject to process and measurement noise; 3) the validation of the proposed chance-constrained MPC with a simulated fleet of quadrotor unmanned aerial vehicles (UAVs).

Notation. In the following, \mathbb{R} is the set of the real numbers. The matrices $\mathbf{0}_{n \times m}$ and $\mathbf{1}_{n \times m}$ are the matrices of size $n \times m$ filled with zeros and ones respectively. The matrix \mathbf{I}_n is the identity matrix of size $n \times n$. The transpose of the matrix \mathbf{A} is denoted by \mathbf{A}^\top . A matrix $\text{diag}(a_1, \dots, a_n)$ is the diagonal matrix with diagonal elements a_1, \dots, a_n . The vector $|\mathbf{x}|$ contains the absolute value of each element of \mathbf{x} . The Euclidean norm of the vector \mathbf{x} is $\|\mathbf{x}\|_2^2 = \mathbf{x}^\top \mathbf{x}$. The notation $\mathbf{A} \succeq 0$ (resp. $\mathbf{A} \succ 0$) means that \mathbf{A} is a positive semidefinite (resp. positive definite) matrix. The matrix $\mathbf{A} \otimes \mathbf{B}$ is the Kronecker product of the matrices \mathbf{A} and \mathbf{B} . If \mathbf{r} is a random variable, then $\mathbb{E}(\mathbf{r})$ is the expected value of \mathbf{r} and $\mathbb{P}(\mathbf{r} \leq \alpha)$ is the probability of the event $\mathbf{r} \leq \alpha$, $\boldsymbol{\mu}_r$ and $\boldsymbol{\Sigma}_r$ are respectively the mean and covariance of \mathbf{r} . The set of all integers from n to m is denoted by $\overline{n, m}$.

2. PROBLEM FORMULATION

In the context of a homogeneous multi-agent system¹ composed of N agents, this section presents the general model of an agent $i \in \overline{1, N}$ subject to process noise and measurement noise. Then, it introduces the control objective of the considered multi-agent system.

2.1 System model

An agent $i \in \overline{1, N}$ obeys the continuous-time linear time invariant dynamics:

$$\begin{aligned} \dot{\mathbf{x}}_i(t) &= \mathbf{A}_C \mathbf{x}_i(t) + \mathbf{B}_C \mathbf{u}_i(t) + \mathbf{d}_i(t) \\ \mathbf{y}_i(t) &= \mathbf{C} \mathbf{x}_i(t) + \boldsymbol{\gamma}_i(t) \end{aligned} \quad (1)$$

with $\mathbf{x}_i \in \mathbb{R}^n$ the state vector, $\mathbf{u}_i \in \mathbb{R}^m$ the input vector, $\mathbf{y}_i \in \mathbb{R}^p$ the output vector, $\mathbf{d}_i \in \mathbb{R}^n$ the process noise, $\boldsymbol{\gamma}_i \in \mathbb{R}^p$ the measurement noise and \mathbf{A}_C , \mathbf{B}_C and \mathbf{C} matrices of appropriate dimensions. The pairs $(\mathbf{A}_C, \mathbf{B}_C)$ and $(\mathbf{A}_C, \mathbf{C})$ are respectively controllable and observable. The system (1) is discretized with the sampling period T_s :

$$\begin{aligned} \mathbf{x}_i(k+1) &= \mathbf{A} \mathbf{x}_i(k) + \mathbf{B} \mathbf{u}_i(k) + \boldsymbol{\delta}_i(k) \\ \mathbf{y}_i(k) &= \mathbf{C} \mathbf{x}_i(k) + \boldsymbol{\gamma}_i(k) \end{aligned} \quad (2)$$

with $\mathbf{A} = \exp(\mathbf{A}_C \cdot T_s)$, $\mathbf{B} = \int_0^{T_s} \exp(\mathbf{A}_C \cdot \tau) \mathbf{B} d\tau$, $\boldsymbol{\delta}_i(k) = \int_0^{T_s} \exp(\mathbf{A}_C \cdot \tau) \mathbf{d}_i((k+1)T_s - \tau) d\tau$.

Assumption 1. The process noise $\mathbf{d}_i(t) = \mathbf{p}(t) + \mathbf{w}_i(t)$, where $\mathbf{p}(t)$ is an external perturbation and $\mathbf{w}_i(t)$ represents the modeling errors, and the measurement noise $\boldsymbol{\gamma}_i(k)$ are independent and normally distributed with means $\boldsymbol{\mu}_d(t) = \mathbf{p}(t)$ and $\boldsymbol{\mu}_\gamma(k) = \mathbf{0}_{p \times 1}$ and covariance matrices $\boldsymbol{\Sigma}_d = \boldsymbol{\Sigma}_w \succ 0$ and $\boldsymbol{\Sigma}_\gamma \succ 0$, respectively². The value of $\mathbf{p}(t)$ is known at each time instant.

For all the agents, the pair (\mathbf{A}, \mathbf{C}) is assumed to be observable. Let $\mathbf{L} \in \mathbb{R}^{n \times m}$ be the gain of a Luenberger observer such that $\mathbf{A}_L = \mathbf{A} - \mathbf{L}\mathbf{C}$ is stable. The dynamics of the estimated state $\widehat{\mathbf{x}}_i(k)$ is:

$$\begin{aligned} \widehat{\mathbf{x}}_i(k+1) &= \mathbf{A} \widehat{\mathbf{x}}_i(k) + \mathbf{B} \mathbf{u}_i(k) + \mathbf{L} (\mathbf{y}_i(k) - \widehat{\mathbf{y}}_i(k)) \\ \widehat{\mathbf{y}}_i(k) &= \mathbf{C} \widehat{\mathbf{x}}_i(k) \end{aligned} \quad (3)$$

The estimation error $\boldsymbol{\varepsilon}_i(k) = \mathbf{x}_i(k) - \widehat{\mathbf{x}}_i(k)$ has for dynamics:

$$\boldsymbol{\varepsilon}_i(k+1) = \mathbf{A}_L \boldsymbol{\varepsilon}_i(k) + \boldsymbol{\delta}_i(k) - \mathbf{L} \boldsymbol{\gamma}_i(k) \quad (4)$$

with the covariance matrix of the initial estimation error chosen such that $\boldsymbol{\Sigma}_\varepsilon(0) \succ 0$. By introducing $\boldsymbol{\varepsilon}_i(k)$ in (3):

$$\widehat{\mathbf{x}}_i(k+1) = \mathbf{A} \widehat{\mathbf{x}}_i(k) + \mathbf{B} \mathbf{u}_i(k) + \mathbf{L} \mathbf{C} \boldsymbol{\varepsilon}_i(k) + \mathbf{L} \boldsymbol{\gamma}_i(k). \quad (5)$$

Proposition 1. The covariance matrix $\boldsymbol{\Sigma}_\delta$ of $\boldsymbol{\delta}_i(k)$ is positive definite and the covariance matrix $\boldsymbol{\Sigma}_\varepsilon(k)$ of the estimation error $\boldsymbol{\varepsilon}_i(k)$ is positive definite $\forall k > 0$.

Proof. The covariance matrix $\boldsymbol{\Sigma}_\delta$ is such that $\boldsymbol{\Sigma}_\delta = \int_0^{T_s} \exp(\mathbf{A}_C \cdot \tau) \boldsymbol{\Sigma}_d \exp(\mathbf{A}_C^\top \cdot \tau) d\tau$ (Franklin et al., 1998). The matrix $\exp(\mathbf{A}_C \cdot t)$ has full rank for all t (Horn and Johnson, 1990) and, by Assumption 1, $\boldsymbol{\Sigma}_d \succ 0$, thus $\boldsymbol{\Sigma}_\delta \succ 0$ (Horn and Johnson, 1990). At time $k > 0$, the random vectors $\boldsymbol{\varepsilon}_i(k-1)$, $\boldsymbol{\delta}_i(k-1)$ and $\boldsymbol{\gamma}_i(k-1)$ are independent. From (4), the covariance matrix of $\boldsymbol{\varepsilon}_i(k)$ is $\boldsymbol{\Sigma}_\varepsilon(k) = \mathbf{A}_L \boldsymbol{\Sigma}_\varepsilon(k-1) \mathbf{A}_L^\top + \boldsymbol{\Sigma}_\delta + \mathbf{L} \boldsymbol{\Sigma}_\gamma \mathbf{L}^\top \succeq 0$ (Horn and Johnson, 1990). Since $\boldsymbol{\Sigma}_\delta \succ 0$, $\boldsymbol{\Sigma}_\varepsilon(k) \succ 0$. \square

2.2 Control objective

The state vector of an agent is $\mathbf{x}_i = [x_i \ \mathbf{x}_{1,i}^\top \ y_i \ \mathbf{x}_{2,i}^\top]^\top$ with $[x_i \ y_i]^\top$ the position of the agent in the two-dimensional plane \mathbb{R}^2 , $\mathbf{x}_{1,i} \in \mathbb{R}^{n_1}$ and $\mathbf{x}_{2,i} \in \mathbb{R}^{n_2}$ possible additional states (e.g. speed) such that $n_1 + n_2 + 2 = n$. Denote by $\mathbb{W} \subset \mathbb{R}^2$ the convex bounded deployment region. The position of each agent belongs to \mathbb{W} , i.e. the restriction $\mathbf{x}_i^r = [x_i \ y_i]^\top$

¹ A homogeneous MAS is considered to simplify the reading of the paper. However, the results can be extended to the case of heterogeneous MAS.

² These means and covariances are considered to be the same for all the agents. However, the result can be generalized to the heterogeneous case where the means and covariances are different for each agent.

of \mathbf{x}_i is such that $\mathbf{x}_i^r \in \mathbb{W}$. This region is divided into N Voronoi cells, one for each agent, such that $\mathbb{W} = \bigcup_{i=1}^N \mathbb{V}_i(k)$ and $\mathbb{V}_i(k) \cap \mathbb{V}_j(k) = \emptyset$, $\forall i, j \in \overline{1, N}$, $i \neq j$. The Voronoi cell of an agent i is the convex bounded polygon defined as $\mathbb{V}_i(k) = \{\mathbf{x} \in \mathbb{W} \mid \|\mathbf{x}_i^r(k) - \mathbf{x}\|_2 \leq \|\mathbf{x}_j^r(k) - \mathbf{x}\|_2, \forall i \neq j\}$ where $\mathbf{x}_i^r(k)$ and $\mathbf{x}_j^r(k)$ are the restrictions of the state vectors $\mathbf{x}_i(k)$, $\mathbf{x}_j(k) \in \mathbb{R}^n$ of agents i and j . As a convex bounded polygon, the Voronoi cell of the agent i is the set:

$$\mathbb{V}_i(k) = \{\mathbf{x} \in \mathbb{W} \mid \mathbf{H}_{i, \mathbb{W}}(k) \mathbf{x} \leq \boldsymbol{\theta}_i(k)\} \quad (6)$$

where $\mathbf{H}_{i, \mathbb{W}}(k) \in \mathbb{R}^{s \times 2}$ and $\boldsymbol{\theta}_i(k) \in \mathbb{R}^s$, with s the number of sides of the cell.

Assumption 2. Each agent is equipped with sensors allowing it to know the other agents positions and is then able to compute its own Voronoi cell.

The Chebyshev center $\mathbf{c}_i(k)$ of the cell $\mathbb{V}_i(k)$ is the center of the largest disc lying in $\mathbb{V}_i(k)$. This center is obtained by a linear optimization problem maximizing the value of the disc's radius such that the radius is positive and each point of the disc is in the cell (Chevet et al., 2020).

The objective is then the deployment of the multi-agent system inside a bounded convex polygon \mathbb{W} into a static configuration such that the agents' positions are at the Chebyshev centers of their Voronoi cells despite the considered process noise and measurement noise acting on the MAS. Each agent computes its own control signal and is driven towards an objective point $(\mathbf{x}_i^0(k), \mathbf{u}_i^0(k))$ solution of $\mathbf{x}_i^0(k) = \mathbf{A} \mathbf{x}_i^0(k) + \mathbf{B} \mathbf{u}_i^0(k)$ such that the restriction of $\mathbf{x}_i^0(k)$ to the position in the plane \mathbb{R}^2 is equal to the Chebyshev center of its Voronoi cell. Moreover, an extended Voronoi cell $\mathbb{V}_{i, \mathbf{x}}(k) = \{\mathbf{x} \in \mathbb{R}^n \mid \mathbf{H}_i(k) \mathbf{x} \leq \boldsymbol{\theta}_i(k)\}$ can be defined with $\mathbf{H}_i(k) \in \mathbb{R}^{s \times n}$. Given the shape of the state vector, the matrix \mathbf{H}_i is obtained by adding n_1 columns of zeros after the first column of $\mathbf{H}_{i, \mathbb{W}}$ and n_2 columns of zeros after the second column of $\mathbf{H}_{i, \mathbb{W}}$. The matrix \mathbf{H}_i and the vector $\boldsymbol{\theta}_i$ will then be used as a polyhedral constraint on the state vector for the MPC problem³.

Since the positions of the agents evolve over time, the Voronoi cells and their associated Chebyshev centers are time-varying. With a state-feedback control law, the nominal multi-agent system has been shown to converge towards a static Chebyshev configuration (Hatleskog et al., 2018). Nevertheless, in the presence of process noise modeled as additive Gaussian noise, a robust control algorithm is required in order to ensure the noise rejection and the multi-agent system convergence towards a static configuration. The next section then presents a decentralized robust MPC algorithm based on a chance-constrained approach.

3. MAIN RESULT

In this section, a decentralized chance-constrained MPC algorithm is formulated based on the estimation of the agent's state. The useful matrices for the definition of the optimization problem are defined. Then, the cost function and constraints of the optimization problem are expressed with the previously defined matrices. However, due to the presence of stochastic perturbations in the agent's model,

³ Such constraints cause a coupling between the agents, thus the need for a decentralized control algorithm.

the agent is subject to probabilistic constraints. A way to transform these probabilistic constraints into algebraic constraints is finally introduced.

3.1 State prediction

Over a prediction horizon N_p , the estimated state (5) and the estimation error (4) become respectively:

$$\widehat{\mathbf{X}}_i(k) = \mathbf{F} \widehat{\mathbf{x}}_i(k) + \mathbf{G}_u \mathbf{U}_i(k) + \mathbf{G}_\varepsilon \mathbf{E}_i(k) + \mathbf{G}_\gamma \boldsymbol{\Gamma}_i(k) \quad (7)$$

$$\mathbf{E}_i(k+1) = \mathbf{F}_\varepsilon \boldsymbol{\varepsilon}_i(k) + \mathbf{G}_\delta^\varepsilon \boldsymbol{\Delta}_i(k) - \mathbf{G}_\gamma^\varepsilon \boldsymbol{\Gamma}_i(k) \quad (8)$$

with $\widehat{\mathbf{X}}_i(k) = [\widehat{\mathbf{x}}_i(k+1)^\top \cdots \widehat{\mathbf{x}}_i(k+N_p)^\top]^\top$, $\mathbf{U}_i(k) = [\mathbf{u}_i(k)^\top \cdots \mathbf{u}_i(k+N_p-1)^\top]^\top$ and $\mathbf{E}_i(k)$ (resp. $\boldsymbol{\Gamma}_i(k)$ and $\boldsymbol{\Delta}_i(k)$) defined the same way as $\mathbf{U}_i(k)$ by replacing \mathbf{u}_i by $\boldsymbol{\varepsilon}_i$ (resp. $\boldsymbol{\gamma}_i$ and $\boldsymbol{\delta}_i$). The matrix \mathbf{F} is such that $\mathbf{F} = [\mathbf{A}^\top \cdots \mathbf{A}^{N_p \top}]^\top$ and the matrix \mathbf{F}_ε is obtained by replacing \mathbf{A} by \mathbf{A}_L in \mathbf{F} . The matrix \mathbf{G}_u is such that:

$$\mathbf{G}_u = \begin{bmatrix} \mathbf{B} & \mathbf{0}_{n \times m} & \cdots & \mathbf{0}_{n \times m} \\ \vdots & \ddots & \ddots & \vdots \\ \vdots & & \ddots & \mathbf{0}_{n \times m} \\ \mathbf{A}^{N_p-1} \mathbf{B} & \cdots & \cdots & \mathbf{B} \end{bmatrix}, \quad (9)$$

the matrices \mathbf{G}_ε and \mathbf{G}_γ are obtained by replacing \mathbf{B} in (9) respectively by $\mathbf{L}\mathbf{C}$ and \mathbf{L} , and the matrices $\mathbf{G}_\delta^\varepsilon$ and $\mathbf{G}_\gamma^\varepsilon$ are obtained by replacing \mathbf{A} by \mathbf{A}_L and \mathbf{B} respectively by \mathbf{I}_n and \mathbf{L} .

3.2 Chance-constrained MPC problem

Based on (Gavilan et al., 2012), a decentralized robust chance-constrained model predictive controller for an agent $i \in \overline{1, N}$ following the dynamics (2) is expressed as follows:

$$\min_{\mathbf{U}_i(k)} J(k) \quad (10a)$$

$$\text{s.t.} \quad \widehat{\mathbf{x}}_i(k+l) \in \mathbb{V}_{i, \mathbf{x}}(k), \quad l \in \overline{1, N_p}, \quad (10b)$$

$$\mathbf{U}_i(k) \in \mathcal{U}_i, \quad (10c)$$

with $J(k) = \mathbb{E} \left(\widehat{\mathbf{X}}_i^{\text{obj}}(k)^\top \mathbf{Q} \widehat{\mathbf{X}}_i^{\text{obj}}(k) + \mathbf{U}_i(k)^\top \mathbf{R} \mathbf{U}_i(k) \right)$.

The weights \mathbf{Q} , $\mathbf{R} \succ 0$ are diagonal matrices and $\widehat{\mathbf{X}}_i^{\text{obj}}(k) = \widehat{\mathbf{X}}_i(k) - \mathbf{X}_i^0$, where $\mathbf{X}_i^0 = \mathbf{1}_{N_p} \otimes \mathbf{x}_i^0(k)$ with $\mathbf{x}_i^0(k)$ the objective state vector defined in Section 2.2. For a vehicle, \mathbf{u}_i^0 is often the null vector, thus it is not considered here. If $\mathbf{u}_i^0 \neq \mathbf{0}_{m \times 1}$, then $\mathbf{U}_i(k)$ is replaced in (10a) by $\mathbf{U}_i(k) - \mathbf{U}_i^0(k)$, where $\mathbf{U}_i^0(k) = \mathbf{1}_{N_p} \otimes \mathbf{u}_i^0(k)$.

Due to stochastic process and measurement noise, solving the optimization problem (10) requires to find a bound for the unknown terms appearing in the constraint (10b) as detailed hereafter. In Section 3.3, this bound is the solution of an optimization problem under probabilistic constraints.

Given the expression of $\widehat{\mathbf{X}}_i(k)$ from (7), the cost function (10a) is rewritten by removing the terms that do not depend on $\mathbf{U}_i(k)$ and have no influence on the solution of (10):

$$J(k) = \mathbf{U}_i(k)^\top (\mathbf{G}_u^\top \mathbf{Q} \mathbf{G}_u + \mathbf{R}) \mathbf{U}_i(k) + 2(\mathbf{F} \widehat{\mathbf{x}}_i(k) + \mathbf{G}_\varepsilon \boldsymbol{\mu}_E(k) - \mathbf{X}_i^0)^\top \mathbf{Q} \mathbf{G}_u \mathbf{U}_i(k) \quad (11)$$

with $\boldsymbol{\mu}_E(k) = \mathbb{E}(\mathbf{E}_i(k))$. Since $\boldsymbol{\mu}_\gamma(k) = \mathbf{0}_{p \times 1}$, the mean of $\boldsymbol{\Gamma}_i(k)$ is the null vector and it does not appear in the expression of the cost function $J(k)$.

The extended Voronoi cell is such that $\mathbb{V}_{i,\mathbf{x}}(k) = \{\mathbf{x} \in \mathbb{R}^n | \mathbf{H}_i(k)\mathbf{x} \leq \boldsymbol{\theta}_i(k)\}$ as detailed in Section 2.2. To predict the evolution of the Voronoi cells over the prediction horizon, each agent would have to know at each time instant the input sequence of all the other agents. With Assumption 2, there is no need of communication between the agents. The extended Voronoi cell of each agent is then considered constant over the prediction horizon. Thus, the constraint (10b) can be rewritten over the prediction horizon by using (7) and replacing $\widehat{\mathbf{X}}(k)$ by its expression:

$$\mathbf{H}_{i,u}(k)\mathbf{G}_u\mathbf{U}_i(k) \leq \boldsymbol{\theta}_{i,u}(k) - \mathbf{H}_{i,u}(k)\mathbf{F}\widehat{\mathbf{x}}_i(k) - \mathbf{H}_{i,u}(k)(\mathbf{G}_\varepsilon\mathbf{E}_i(k) + \mathbf{G}_\gamma\boldsymbol{\Gamma}_i(k)) \quad (12)$$

where $\mathbf{H}_{i,u} = \mathbf{I}_{N_p} \otimes \mathbf{H}_i$ and $\boldsymbol{\theta}_{i,u} = \mathbf{1}_{N_p} \otimes \boldsymbol{\theta}_i$.

In the constraint (10c), \mathbb{U}_i is a set of polyhedral constraints such that $\mathbb{U}_i = \{\mathbf{u} \in \mathbb{R}^{m_{N_p}} | \|\mathbf{u}\| \leq \mathbf{U}_{\max}\}$, where $\mathbf{U}_{\max} \in \mathbb{R}^{m_{N_p}}$ with only positive components.

With this formulation, the constraint (12) depends on the knowledge of the process noise and the measurement noise over the prediction horizon. However, the value of these signals is not known and the only available information are the mean and covariance of these noises. The constraint (12) then needs to be modified to depend only on the available information in order to solve the problem (10).

3.3 Noise bound for robust satisfaction of constraints

In (12), a bound for the uncertain term $\mathbf{H}_{i,u}(k)(\mathbf{G}_\varepsilon\mathbf{E}_i(k) + \mathbf{G}_\gamma\boldsymbol{\Gamma}_i(k))$, which is also written $\mathbf{H}_{i,u}(k)[\mathbf{G}_\varepsilon \ \mathbf{G}_\gamma]\boldsymbol{\Xi}_i(k)$, with $\boldsymbol{\Xi}_i(k) = [\mathbf{E}_i(k)^\top \ \boldsymbol{\Gamma}_i(k)^\top]^\top$ the disturbance vector, has to be found in order to express the constraint (12) only based on known information.

If the disturbance vector $\boldsymbol{\Xi}_i(k)$ is normally distributed with mean $\boldsymbol{\mu}_\Xi(k)$ and covariance matrix $\boldsymbol{\Sigma}_\Xi(k)$, then:

$$\mathbf{Y}_i(k) = (\boldsymbol{\Xi}_i(k) - \boldsymbol{\mu}_\Xi(k))^\top \boldsymbol{\Sigma}_\Xi^{-1}(k) (\boldsymbol{\Xi}_i(k) - \boldsymbol{\mu}_\Xi(k)) \quad (13)$$

follows a chi-squared law with $(n+p)N_p$ degrees of freedom (Flury, 1997), where $(n+p)N_p$ is the size of $\boldsymbol{\Xi}_i(k)$. Then, finding the solution α of the chance constraint $\mathbb{P}(\chi^2((n+p)N_p) \leq \alpha) = P$ ensures that $\mathbf{Y}_i(k)$ is bounded by α with a probability P (Gavilan et al., 2012).

The objective is then to find a bound $\mathbf{b}_i(k)$ such that $\mathbf{b}_i(k) \leq -\mathbf{M}_i\boldsymbol{\Xi}_i(k)$, where $\mathbf{M}_i = \mathbf{H}_{i,u}(k)[\mathbf{G}_\varepsilon \ \mathbf{G}_\gamma]$, with a probability P close to one. With this bound, the constraint (12) is satisfied for almost all disturbances. This bound is:

$$\begin{aligned} (\mathbf{b}_i(k))_l &= \min_{\boldsymbol{\Xi}_i(k)} -(\mathbf{M}_i)_l \boldsymbol{\Xi}_i(k) \\ \text{s.t.} \quad &\mathbf{Y}_i(k) \leq \alpha \end{aligned} \quad (14)$$

where $(\mathbf{M}_i)_l$ and $(\mathbf{b}_i(k))_l$ are respectively the l -th row of \mathbf{M}_i and the l -th element of $\mathbf{b}_i(k)$ and $\mathbf{Y}_i(k)$ defined in (13).

To guarantee the existence of the bound, $\boldsymbol{\Xi}_i(k)$ has to be normally distributed, thus $\boldsymbol{\Sigma}_\Xi$ has to be invertible. Since $\boldsymbol{\varepsilon}_i(k-1)$, $\boldsymbol{\Delta}_i(k-1)$ and $\boldsymbol{\Gamma}_i(k-1)$ are independent, from the expression of $\mathbf{E}_i(k)$ in (8), this covariance is:

$$\boldsymbol{\Sigma}_\Xi(k) = \begin{bmatrix} \boldsymbol{\Sigma}_E(k) & -\mathbf{G}_\gamma^\varepsilon \boldsymbol{\Sigma}_{\Gamma,L} \\ -\boldsymbol{\Sigma}_{\Gamma,L}^\top \mathbf{G}_\gamma^\varepsilon & \boldsymbol{\Sigma}_\Gamma \end{bmatrix} \quad (15)$$

where:

$$\boldsymbol{\Sigma}_E(k) = \mathbf{F}_\varepsilon \boldsymbol{\Sigma}_\varepsilon(k-1) \mathbf{F}_\varepsilon^\top + \mathbf{G}_\delta^\varepsilon \boldsymbol{\Sigma}_\Delta \mathbf{G}_\delta^{\varepsilon\top} + \mathbf{G}_\gamma^\varepsilon \boldsymbol{\Sigma}_\Gamma \mathbf{G}_\gamma^{\varepsilon\top}, \quad (16)$$

with $\boldsymbol{\Sigma}_\Gamma = \mathbf{I}_{N_p} \otimes \boldsymbol{\Sigma}_\gamma$, $\boldsymbol{\Sigma}_\Delta = \mathbf{I}_{N_p} \otimes \boldsymbol{\Sigma}_\delta$ and $\boldsymbol{\Sigma}_{\Gamma,L}$ a block lower diagonal matrix with $\boldsymbol{\Sigma}_\gamma$ the element at line l and column $l-1$, where $l > 1$.

Proposition 2. The covariance matrix $\boldsymbol{\Sigma}_\Xi(k)$ is positive definite $\forall k > 0$.

Proof. By taking the Schur complement (Boyd et al., 1994) in (15), $\boldsymbol{\Sigma}_\Xi(k) \succ 0$ if and only if $\boldsymbol{\Sigma}_\Gamma \succ 0$ (which is always true) and $\mathbf{S}(k) \succ 0$ with $\mathbf{S}(k) = \boldsymbol{\Sigma}_E(k) - \mathbf{G}_\gamma^\varepsilon \boldsymbol{\Sigma}_{\Gamma,L} \boldsymbol{\Sigma}_\Gamma^{-1} \boldsymbol{\Sigma}_{\Gamma,L}^\top \mathbf{G}_\gamma^{\varepsilon\top}$. Since $\boldsymbol{\Sigma}_\gamma \succ 0$, $\boldsymbol{\Sigma}_\gamma$ is invertible and $\boldsymbol{\Sigma}_\Gamma^{-1} = \mathbf{I}_{N_p} \otimes \boldsymbol{\Sigma}_\gamma^{-1}$. Using (16), $\mathbf{S}(k)$ becomes $\mathbf{S}(k) = \mathbf{F}_\varepsilon \boldsymbol{\Sigma}_\varepsilon(k-1) \mathbf{F}_\varepsilon^\top + \mathbf{G}_\delta^\varepsilon \boldsymbol{\Sigma}_\Delta \mathbf{G}_\delta^{\varepsilon\top} + \mathbf{G}_\gamma^\varepsilon \boldsymbol{\Sigma}_{\Gamma,1} \mathbf{G}_\gamma^{\varepsilon\top}$, with $\boldsymbol{\Sigma}_{\Gamma,1} = \text{diag}(\boldsymbol{\Sigma}_\gamma, \mathbf{0}_{(p-1)N_p \times (p-1)N_p})$. To have $\mathbf{S}(k) \succ 0$, at least one of the matrices defining $\mathbf{S}(k)$ has to be positive definite while the others only need to be positive semidefinite. Proposition 1 gives $\boldsymbol{\Sigma}_\varepsilon(k-1) \succ 0$ thus $\mathbf{F}_\varepsilon \boldsymbol{\Sigma}_\varepsilon(k-1) \mathbf{F}_\varepsilon^\top \succeq 0$ (Horn and Johnson, 1990). Since $\boldsymbol{\Sigma}_{\Gamma,1} \succeq 0$, it is verified that $\mathbf{G}_\gamma^\varepsilon \boldsymbol{\Sigma}_{\Gamma,1} \mathbf{G}_\gamma^{\varepsilon\top} \succeq 0$. It remains to prove that $\mathbf{G}_\delta^\varepsilon \boldsymbol{\Sigma}_\Delta \mathbf{G}_\delta^{\varepsilon\top} \succ 0$. The matrix $\mathbf{G}_\delta^\varepsilon$ defined in Section 3.1 is $\mathbf{G}_\delta^\varepsilon = \mathbf{I}_{nN_p} + \mathbf{T}$ where \mathbf{T} is a strictly lower triangular matrix. Thus, $\mathbf{G}_\delta^\varepsilon \boldsymbol{\Sigma}_\Delta \mathbf{G}_\delta^{\varepsilon\top} = \boldsymbol{\Sigma}_\Delta + \mathbf{T} \boldsymbol{\Sigma}_\Delta \mathbf{T}^\top + \mathbf{T} \boldsymbol{\Sigma}_\Delta + \boldsymbol{\Sigma}_\Delta \mathbf{T}^\top$, with the last two terms positive semidefinite because $\boldsymbol{\Sigma}_\Delta$ is a block diagonal matrix and \mathbf{T} is strictly lower triangular, thus their eigenvalues are all 0. In addition, $\mathbf{T} \boldsymbol{\Sigma}_\Delta \mathbf{T}^\top \succeq 0$ and $\boldsymbol{\Sigma}_\Delta \succ 0$ thus $\boldsymbol{\Sigma}_\Xi(k) \succ 0$. \square

With Proposition 2, $\boldsymbol{\Sigma}_\Xi(k)$ is invertible. By applying a similar procedure to the one presented in (Gavilan et al., 2012), the optimization problem (14) is explicitly solved and the l -th element of $\mathbf{b}_i(k)$ is:

$$(\mathbf{b}_i(k))_l = -\sqrt{(\mathbf{M}_i)_l \boldsymbol{\alpha} \boldsymbol{\Sigma}_\Xi(k) (\mathbf{M}_i)_l^\top} - (\mathbf{M}_i)_l \boldsymbol{\mu}_\Xi(k). \quad (17)$$

Then, by replacing the constraint (10b) by (12) with the bound defined in (17), it is now possible to find a solution to the proposed decentralized CCMPC (10).

4. SIMULATIONS

In this paper, the considered multi-agent system is a fleet of four quadrotor UAVs. The nonlinear continuous-time state-space model of a UAV agent is presented in (Chevet et al., 2020). This model is the one used to simulate the behavior of an agent. The control architecture for this system is as follows: a position reference is provided to the position controller which computes pitch and roll references for the orientation controller. The yaw reference is constant during the flight. Then, the orientation and the altitude controllers provide torque and upward thrust inputs to the nonlinear UAV model. The chance-constrained MPC algorithm described in Section 3 is used for the position controller, while the orientation and altitude controllers are obtained by feedback linearization as in (Voos, 2009).

4.1 Position subsystem model

To design the position controller, the position subsystem is obtained from the linearized and discretized state-space model (Chevet et al., 2020) to fit the system (2). For one UAV agent, the state vector is $\mathbf{x}_i = [x_i \ v_{x,i} \ y_i \ v_{y,i}]^\top$, with $i \in \overline{1,4}$, x_i, y_i the agent's position and $v_{x,i}, v_{y,i}$ the

components of its horizontal speed. The input vector is $\mathbf{u}_i = [\phi_i \ \theta_i]^\top$, with ϕ_i and θ_i the agent's roll and pitch angles. The yaw reference remains equal to 0° during the flight, thus the state matrices defined in (2) are:

$$\mathbf{A} = \mathbf{I}_2 \otimes \begin{bmatrix} 1 & T_s \\ 0 & 1 \end{bmatrix} \quad \mathbf{B} = \frac{1}{2}gT_s \begin{bmatrix} 0 & 1 \\ -1 & 0 \end{bmatrix} \otimes \begin{bmatrix} T_s \\ 2 \end{bmatrix}, \quad (18)$$

$$\mathbf{C} = \mathbf{I}_2 \otimes [1 \ 0]$$

with $g = 9.81 \text{ m} \cdot \text{s}^{-2}$ the gravitational acceleration and T_s the sampling period. The noise covariances are $\Sigma_d = \text{diag}(0.001, 0.025, 0.001, 0.025)$ and $\Sigma_\gamma = 0.0011 \cdot \mathbf{I}_2$ and μ_d will be described in Section 4.4.

4.2 Position controller

The chance-constrained model predictive controller runs at $T_s^{\text{out}} = 0.2 \text{ s}$ with a prediction horizon $N_p = 10$, while the inner loop (the orientation controller) runs at $T_s^{\text{in}} = 0.001 \text{ s}$. Thus, to accurately estimate the system's state, the structure from Fig. 1 is used. On a real UAV, the variation rate of the angle reference is limited to avoid important variations on the actuators' inputs. Thus, here, the variation rate of the angle reference is limited to $\pm 100^\circ/\text{s}$. Then, this reference $[\phi_i^{\text{ref}}(k) \ \theta_i^{\text{ref}}(k)]^\top$ is sent to the inner loop controller and an observer, both running at T_s^{in} as shown in Fig. 1. This observer is meant to provide an accurate value of the state to the outer loop controller and thus runs at the same rate as the inner loop controller. The state estimate is then sent to the position controller every T_s^{out} seconds.

With this structure, the prediction model (3) considered for the chance-constrained MPC design uses the matrices in (18) with $T_s = T_s^{\text{out}}$, while the second observer's model is obtained from the matrices in (18) with $T_s = T_s^{\text{in}}$. The observer gain \mathbf{L} in (3) is a linear quadratic estimator obtained with the weights $\mathbf{Q} = 100\mathbf{I}_4$ and $\mathbf{R} = \mathbf{I}_2$. The observer in Fig. 1 is also a linear quadratic estimator obtained with the weights $\mathbf{Q} = 10\mathbf{I}_4$ and $\mathbf{R} = \mathbf{I}_2$.

The objective point $\mathbf{x}_i^0(k)$ is a vector with four elements: the coordinates of the Chebyshev center of the cell as first and third elements and zeros as second and fourth elements. Moreover, the weights \mathbf{Q} and \mathbf{R} for the cost function (10a) are chosen to be $\mathbf{Q} = \mathbf{I}_{N_p} \otimes \text{diag}(10, 1, 10, 1)$ and $\mathbf{R} = 100\mathbf{I}_{2N_p}$. The angle reference is limited to $\pm 30^\circ$ such that $\mathbf{U}_i = \{\mathbf{u} \in \mathbb{R}^{2N_p} \mid \|\mathbf{u}\| \leq \pi/6 \cdot \mathbf{1}_{2N_p}\}$.

Finally, with the considered dimensions for the problem, the chi-squared variable presented in Section 3.3 has 60 degrees of freedom. Thus, if P is chosen to be 0.999, nearly all the disturbances are bounded by $\alpha = 99.607$ in (14).

4.3 Orientation and altitude controllers

The following orientation and altitude controllers are obtained as presented in (Voos, 2009). Further description

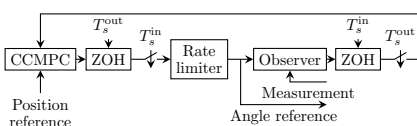


Fig. 1. Structure of the position controller.

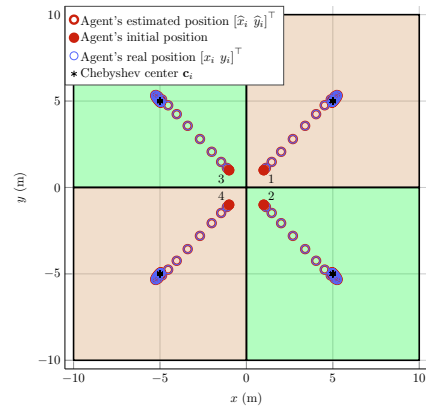


Fig. 2. Evolution of the agents' real and estimated position and Chebyshev center from $t = 0 \text{ s}$ to $t = 9.8 \text{ s}$.

is out of the scope of this paper and these are given for reproducibility of the results. The torque on the x axis is computed as $\tau_{x,i}(k) = (I_z - I_y)\omega_{y,i}(k)\omega_{z,i}(k) + I_x K_1 \omega_{x,i}(k) + K_2 (\phi_i^{\text{ref}}(k) - \phi_i(k))$ where $\omega_{x,i}$, $\omega_{y,i}$ and $\omega_{z,i}$ are the angular speeds $I_x = I_y = 0.03 \text{ kg} \cdot \text{m}^2$ and $I_z = 0.04 \text{ kg} \cdot \text{m}^2$ are the moments of inertia along the three axes and K_1 and K_2 are parameters chosen to obtain the desired dynamics for the inner loop. Here, the values $K_1 = -200$ and $K_2 = 100$ are considered for the parameters. The torques $\tau_{y,i}(k)$ and $\tau_{z,i}(k)$ are obtained with a cyclic permutation of x , y and z in the expression of $\tau_{x,i}(k)$ and by replacing ϕ by θ and ψ (the yaw angle) respectively, with $\psi_i^{\text{ref}}(k) = 0$. With the same approach, the total upward thrust is $F_{t,i}(k) = m \cdot (g + K_3 v_{z,i}(k) + K_4 (z_i^{\text{ref}}(k) - z_i(k)))/(\cos \phi_i(k) \cos \theta_i(k))^{-1}$ where z_i and $v_{z,i}$ are the altitude and vertical speed, z_i^{ref} is the altitude reference, $m = 1.4 \text{ kg}$ is the mass of the UAV and K_3 and K_4 are parameters chosen to obtain the desired dynamics for the altitude loop. Here, the values $K_3 = -3.6$ and $K_4 = 4$ are considered for the parameters.

4.4 Simulation results

A fleet of four quadrotor UAVs is deployed inside a square of 20 m of side length: $\mathbb{W} = \{\mathbf{x} \in \mathbb{R}^2 \mid |\mathbf{x}| \leq 10 \cdot \mathbf{1}_2\}$. They all start from a hovering position with $z_i(0) = 5 \text{ m}$, with $i \in \overline{1,4}$, at $\mathbf{x}_1(0) = [1 \ 0 \ 1 \ 0]^\top$, $\mathbf{x}_2(0) = [1 \ 0 \ -1 \ 0]^\top$, $\mathbf{x}_3(0) = [-1 \ 0 \ 1 \ 0]^\top$, $\mathbf{x}_4(0) = [-1 \ 0 \ -1 \ 0]^\top$.

At $t = 0 \text{ s}$, they start tracking the Chebyshev center of their associated Voronoi cell and are subject to a process noise and a measurement noise having a mean $\mu_d(t) = \mu_\gamma(k) = \mathbf{0}_{4 \times 1}$ and the covariances Σ_δ and Σ_γ described in Section 4.1. From $t = 12 \text{ s}$ to $t = 20 \text{ s}$, each UAV is subject to a wind gust of 2 m/s on each axis such that $\mu_d(t) = [0 \ 2 \ 0 \ 2]^\top$ which is assumed to be known by the agents as stated in Assumption 1.

The first part of the movement, from $t = 0 \text{ s}$ to $t = 9.8 \text{ s}$, is shown in Fig. 2. The initial positions $[x_i(0) \ y_i(0)]^\top$ are represented by discs (red discs). The evolution of the real positions $[x_i \ y_i]^\top$ (blue circles) as well as the evolution of the estimated positions $[\hat{x}_i \ \hat{y}_i]^\top$ (red circles) and the Chebyshev centers \mathbf{c}_i (black asterisks) of the four agents every 0.2 s are presented inside the Voronoi partition at

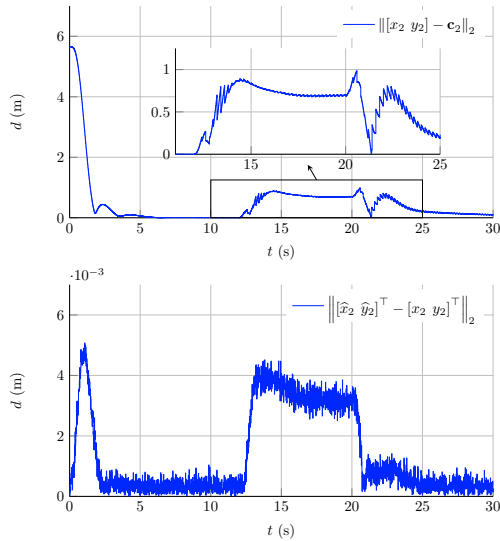


Fig. 3. Distance between the agent 2 real position and its Chebyshev center (top) and between the agent 2 real position and its estimated position (bottom).

$t = 9.8$ s. The position of each agent converges to its Chebyshev center as expected from (Hatleskog et al., 2018), while the estimated position converges quickly to the real position. In the following, since the formation is symmetric, only the results for the agent 2 are provided, the results for the other agents being similar.

Figure 3 presents the distance between the real position $[x_2 \ y_2]^T$ of agent 2 and its Chebyshev center \mathbf{c}_2 and the distance between the real position and the estimated position $[\hat{x}_2 \ \hat{y}_2]^T$ of agent 2. The estimated position is initialized to the agent's real position. The bottom plot of Fig. 3 shows that the estimation error is relatively small ($\|\varepsilon_2(k)\|_2 < 6 \cdot 10^{-3}$) during the entire movement.

The top plot of Fig. 3 shows that the agent converges to its Chebyshev center since the distance between the real position of agent 2 and \mathbf{c}_2 is close to 0 m after 2 s. However, from $t = 12$ s to $t = 20$ s, the system is subject to wind perturbations. Because there is no integral action in the proposed control algorithm, a static error appears while the system is perturbed. Without perturbation, the agent converges back to its Chebyshev center.

5. CONCLUSION

This paper presents a decentralized chance-constrained model predictive control algorithm with state estimation meant to drive a multi-agent system subject to process noise and measurement noise into a static configuration when deployed inside a bounded convex two-dimensional area. At each time instant, each agent computes a Voronoi cell in which it will evolve and the Chebyshev center of this Voronoi cell. Then, with the proposed approach, the system converges towards a static configuration in which each agent lies on its Chebyshev center despite model mismatch and perturbations (represented respectively by the covariance and the mean of the process noise) and measurement noise. Simulation results show the efficiency of the proposed approach. Future work will extend this result to the case of biased measurements corresponding, for example, to sensor faults.

REFERENCES

- Boyd, S., El Ghaoui, L., Feron, E., and Balakrishnan, V. (1994). *Linear matrix inequalities in system and control theory*. SIAM.
- Chevet, T., Vlad, C., Stoica Maniu, C., and Zhang, Y. (2020). Decentralized MPC for UAVs formation deployment and reconfiguration with multiple outgoing agents. *J. Intell. Robot. Syst.*, 97(1), 155–170.
- Cortes, J., Martinez, S., Karatas, T., and Bullo, F. (2004). Coverage control for mobile sensing networks. *IEEE Trans. Robot. Autom.*, 20(2), 243–255.
- Dai, L., Xia, Y., Gao, Y., and Cannon, M. (2017). Distributed stochastic MPC of linear systems with additive uncertainty and coupled probabilistic constraints. *IEEE Trans. Autom. Control*, 62(7), 3474–3481.
- Farina, M., Giulioni, L., and Scattolini, R. (2016). Stochastic linear model predictive control with chance constraints – A review. *J. Process Control*, 44, 53–67.
- Flury, B. (1997). *A first course in multivariate statistics*. Springer.
- Franklin, G.F., Powell, J.D., Workman, M.L., et al. (1998). *Digital Control of Dynamic Systems*. Addison-Wesley.
- Gavilan, F., Vazquez, R., and Camacho, E.F. (2012). Chance-constrained model predictive control for spacecraft rendezvous with disturbance estimation. *Control Eng. Pract.*, 20(2), 111–122.
- Hatleskog, J., Oлару, S., and Hovd, M. (2018). Voronoi-based deployment of multi-agent system. In *57th CDC*, 5403–5408.
- Horn, R.A. and Johnson, C.R. (1990). *Matrix analysis*. Cambridge University Press.
- Limon, D., Alvarado, I., Alamo, T., and Camacho, E.F. (2010). Robust tube-based MPC for tracking of constrained linear systems with additive disturbances. *J. Process Control*, 20(3), 248–260.
- Ma, L., Wang, Z., Han, Q.L., and Liu, Y. (2017). Consensus control of stochastic multi-agent systems: a survey. *Sci. China Inf. Sci.*, 60(12), 120–201.
- Nguyen, M.T., Stoica Maniu, C., and Oлару, S. (2017). Optimization-based control for multi-agent deployment via dynamic Voronoi partition. *IFAC-PapersOnLine*, 50(1), 1828–1833.
- Petersen, I.R., James, M.R., and Dupuis, P. (2000). Minimax optimal control of stochastic uncertain systems with relative entropy constraints. *IEEE Trans. Autom. Control*, 45(3), 398–412.
- Schwager, M., Rus, D., and Slotine, J.J. (2011). Unifying geometric, probabilistic, and potential field approaches to multi-robot deployment. *Int. J. Robot. Res.*, 30(3), 371–383.
- Sharifi, F., Mirzaei, M., Zhang, Y., and Gordon, B.W. (2015). Cooperative multi-vehicle search and coverage problem in an uncertain environment. *Unmanned Syst.*, 3(1), 35–47.
- Ugrinovskii, V.A. (1998). Robust H infinity control in the presence of stochastic uncertainty. *Int. J. Control*, 71(2), 219–237.
- Voos, H. (2009). Nonlinear control of a quadrotor micro-uav using feedback-linearization. In *IEEE Int. Conf. Mechatronics*, 1–6.
- Voronoi, G. (1908). Nouvelles applications des paramètres continus à la théorie des formes quadratiques. *Journal für die reine und angewandte Mathematik*, 134, 198–287.